Supplementary Information

of

Crown ether-based interface modification for inverted perovskite solar cells with enhanced efficiency and stability

Yang Zhang[a], Ting Jiang[a], Jingquan Zhang [a,b], Lili Wu [a,b], Guanggen Zeng [a,b], Baoyan Fan[c], Komiljon Yakubov[d], Tulkin Nurmurodov[e], Ilyos Rakhmatullaev[f], Xia Hao[a,b,*]

[a] *Institute of New Energy and Low-Carbon Technology & College of Materials Science and Engineering, Sichuan University, Chengdu 610065, China*

[b] *Engineering Research Center of Alternative Energy Materials & Devices, Ministry of Education, Chengdu 610065, China*

[c] *College of Materials and New Energy, Chongqing University of Science and Technology, Chongqing 401331, China*

[d] *Department of Physics, Urgench State University, Urgench 220100, Uzbekistan*

[e] *Department of Chemical Technology, Navoi State University of Mining and Technologies, Navoi 210100, Uzbekistan*

[f] *Department of Mathematics and Physics, Alfraganus University, Tashkent 100190, Uzbekistan*

**Correspondence Information: hao.xia0808@scu.edu.cn (X. Hao)*

Experimental section

Materials and solutions

N,N-dimethylformamide (DMF, 99.8%), dimethyl sulfoxide (DMSO, ≥99.9%), chlorobenzene (CB, ≥99.8%), isopropanol (IPA, ≥99.5%), Dibenzo-18-crown-6 (DB18C6, 98%), and anhydrous ethanol were purchased from Sigma Aldrich. Lead (II) iodide (PbI_2, 99.99%). Cesium iodide (CsI, >99,9%), and [4-(3,6-Dimethyl-9*H*-carbazol-9-yl)butyl]phosphonic acid (Me-4PACz, >99%) were purchased from Tokyo Chemical Industry (TCI). Formamidinium iodid (FAI, >99.99), methylammonium bromide (MABr, >99.99), and methylammonium chloride (MACl, >99%) were purchased from Greatcell Solar Materials Pty. Ltd. Lead bromide ($PbBr_2$, >99.99%), bathocuproine (BCP, 99.5%), and [6,6]-Phenyl C_{61} butyric acid methyl ester (PCBM, 99.0%) were purchased from Xi'an Polymer Light Technology Crop. NiO_x (99.99%) powders and Spiro-OMeTAD (99.9%) were purchased from Advanced Selection Technology Co., Ltd. Silver was purchased from (Zhong Nuo Advanced Material Beijing) Technology Co., Ltd. ITO glass substrates (2.5 cm×2.5 cm) were purchased from Shangyang Technology.

NiO_x was dissolved in deionized water (20 mg/mL). Me-4PACz was dissolved in ethanol (0.5 mg/mL). To prepare perovskite solution, 41.73 mg CsI, 15.55 mg MABr, 55.3 mg $PbBr_2$, 450.8 mg FAI, 1317 mg PbI_2 and 20.34 mg MACl were mixed in 1 mL mixed solvent (DMF:DMSO=4:1) according to a formula of

$Cs_{0.04}(FA_{0.84}MA_{0.16})_{0.96}Pb(I_{0.84}Br_{0.16})_3$. DB18C6 was dissolved in CB (0.5 mg/mL). PCBM was dissolved in CB (15 mg/mL). BCP was dissolved in IPA (0.5 mg/mL).

Device fabrication

The ITO glass substrate was ultrasonically cleaned with water and anhydrous ethanol for 40 min. Then, the cleaned substrate was blown dry by high purity nitrogen, followed treated for 15 min by ultraviolet-ozone (UVO). After that, 120 μL NiO_x solution was spin-coting for 30 s at 2000 rpm and annealing at 150 ℃ for 30 min. After cooling to room temperature, transfer the substrate into nitrogen-filled glove-box. The 100 μL Me-4PACz solution was deposited on NiO_x layer by spin-coating at 3000 rpm for 30 s and annealing at 100 ℃ for 10 min. Then, perovskite film was obtained by spin-coating 1000 rpm for 10 s and 5000 rpm for 40 s and drip 200 μL CB at the 45 s, followed by annealing at 100 ℃ for 30 min. For target, the perovskite film was treated with 80 μL of DB18C6 solution via spin-coating (4000 rpm, 20 s) prior to being annealed at 100 °C for 5 minutes. Afterwards, 85 μL PCBM solution and 105 μL BCP solution were sequentially deposited at 2000 rpm for 30 s and 4000 rpm for 30 s, respectively. Finally, a 120 nm thick film of Ag was evaporated onto the BCP layer.

Characterization

The ultraviolet-visible (UV-Vis) absorption spectra were measured by using Ultraviolet-visible spectrophotometer (Lambda 950) produced by PerkinElmer, Inc. The X-ray diffraction (XRD) patterns were obtained by X-Ray diffractometer (XRD-6100) produced by Shimazu. The scanning electron microscopy (SEM) images were

measured by field emission scanning electron microscope (Hitachi Regulus8100) produced by Hitachi, Japan. The atomic force microscopy (AFM) images were obtained to using atomic force microscope (DI Multimode 8) produced by Bruker Nano Inc, Germany. The X-ray photoelectron spectroscopy (XPS) patterns were conducted by X-ray photoelectron spectroscopy (ESCALAB 250Xi) produced by ThermoFisher. The fourier transform infrared spectroscopy (FTIR) tests were conducted by infrared spectrometer (Nicolet iS50) produced by ThermoFisher. The Stead-state photoluminescence (PL) and time-resolved photoluminescence (TRPL) were conducted by FLS980 produced by Edinburgh. The kelvin probe force microscopy (KPFM) images of perovskite films were measured using Multimode 8 high-resolution scanning probe microscope produced by Bruker. The UV photoelectron spectroscopy (UPS) measurements were conducted through identical equipment with XPS test to obtain the work function and valance band of perovskite films.

The *J-V* curves were measured using a source meter (Keysight Technologies, B2901A) and Sun 200 steady-state solar simulator produced by ABET Technology under simulated sunlight (AM 1.5G, 100 mW/cm^2) calibrated by a standard silicon solar cell (Enli Tech, RC-00205). The external quantum efficiency (EQE) tests were conducted through QE-R Guangyan technology quantum efficiency test system (QE-R3018) produced by Enlitech, calibrated by a standard silicon solar cell. The dark *J-V* and space charge limited current (SCLC) tests were carried out using a Keysight 2400 source meter under dark condition. The light intensity dependence of V_{OC}

measurements were conducted by *J-V* test under different intensity of illumination. The capacitance-voltage (*C-V*) tests were measured by an electrochemical workstation fabricated by LVIUM. The maximum power point tracking (MPPT) was recorded by white LED simulator (Weina Bonuo new materials Co., Ltd., Qingdao) equivalent to 1 sun (100 mW cm^{-2}) in ambient air.

Note S1. Calculation of crystallite sizes

The mean crystallite sizes (D) of the most intense diffraction peak (i.e., (001) facet) of the perovskite are calculated by the Scherrer equation:

$$D = \frac{K\lambda}{FWHM\cos\theta} \quad (1)$$

where K is the Scherrer constant, λ is the wavelength of the x-ray used and θ is the Bragg angle.

Note S2. TRPL characterizations analysis

TRPL is used to investigate the recombination and molecular dynamics of electrons. A double-exponential function is used to fit the curve:

$$y(t) = y_0 + A_1 \exp\left(-\frac{t}{\tau_1}\right) + A_2 \exp\left(-\frac{t}{\tau_2}\right) \quad (2)$$

where τ is decay component, A_1 and A_2 are decay amplitudes. The average lifetime of the nonradiative recombination process can be calculated according to the following formula:

$$\tau_{ave} = \frac{\sum A_i \tau_i^2}{\sum A_i \tau_i} \quad (3)$$

The corresponding fitted parameters are shown in **Table S2**.

Note S3. SCLC analysis

SCLC spectra measurement is performed based on the structure of ITO/NiO_x/Me-4PACz/Perovskite/Spiro-OMeTAD/Au to determine the trap density (n_t). The n_t is calculated using the following equations:

$$n_t = \frac{2V_{TFL}\varepsilon_r\varepsilon_0}{eL^2} \quad (4)$$

where e is the elementary charge, V_{TFL} is the trap-filled limit voltage, L is the thickness of the perovskite film, ε_0 is the vacuum permittivity and ε_r is the relative dielectric constant of perovskite.

Note S4. Calculation of hysteresis index

The hysteresis index (HI) is defined by the formula:

$$HI = \frac{|PCE_{reverse} - PCE_{forward}|}{PCE_{reverse}} \times 100\% \quad (5)$$

where $PCE_{reverse}$ is PCE in the condition of reverse scans in *J-V* test and $PCE_{forward}$ is PCE in the condition of forward scans in *J-V* test.

Note S5. Calculation of ideal factor

The ideal factor (n_{id}) can be obtained from intensity-dependent V_{OC} tests, as calculated as following:

$$V_{OC} = \left(\frac{n_{id}K_BT}{q}\right) \ln\left(\frac{I}{I_0} + 1\right) \quad (6)$$

where K_B is the Boltzmann constant, q is the electron charge, T is the absolute temperature, n_{id} is the ideal factor, I_0 is the initial light intensity and I is the light intensity.

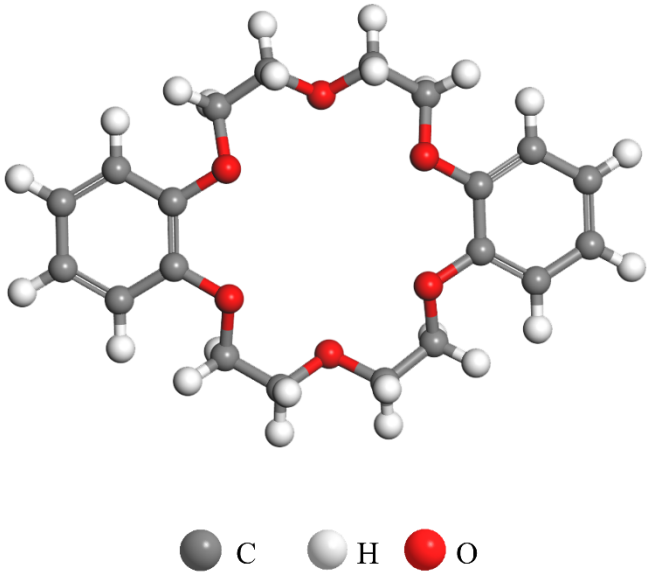

Fig. S1 Molecular structure diagram of DB18C6.

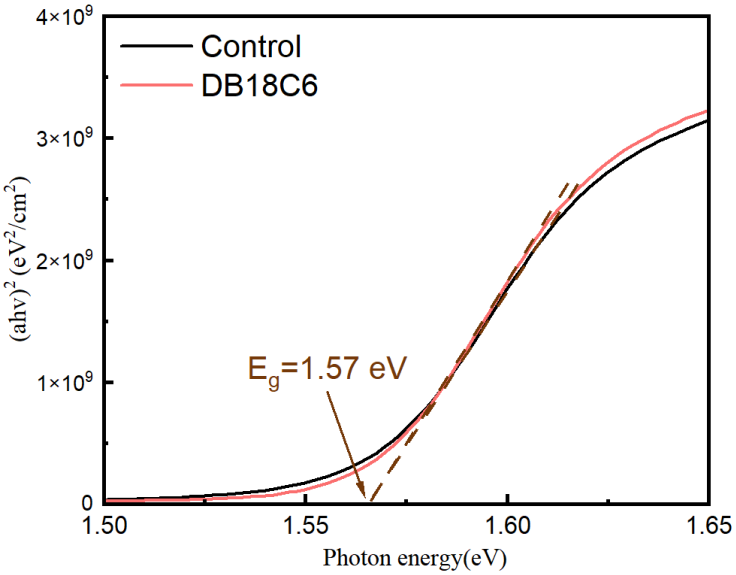

Fig. S2 Tauc plots of the perovskite film before and after DB18C6-modification.

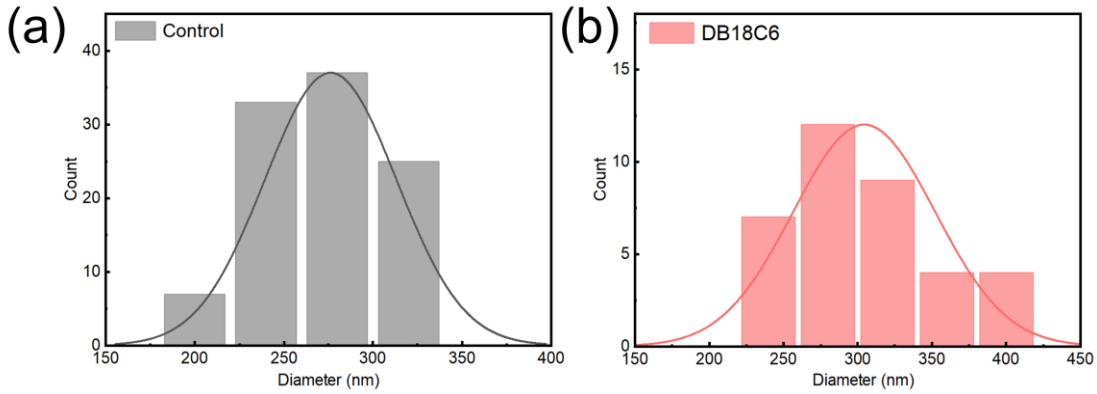

Fig. S3 The particle size distribution statistics in the top-view SEM images of perovskite films: (a) control; (b) target.

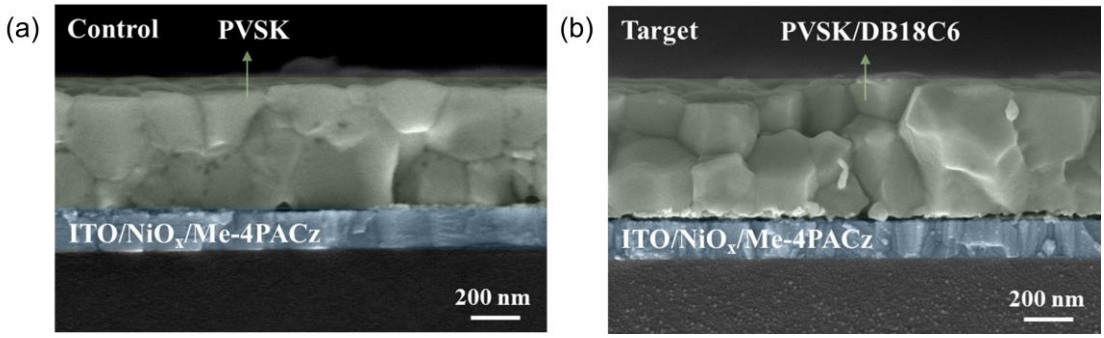

Fig. S4 The cross-sectional SEM images of perovskite film: (a) control; (b) target.

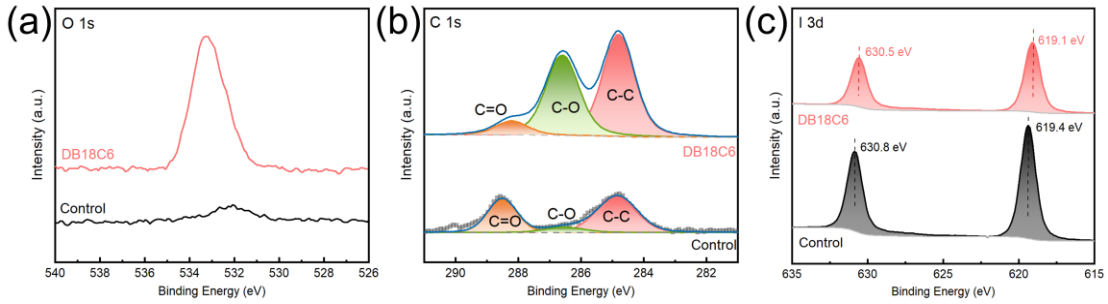

Fig. S5 XPS spectra of the (a) O 1s, (b) C 1s and (c) I 3d of control and target films.

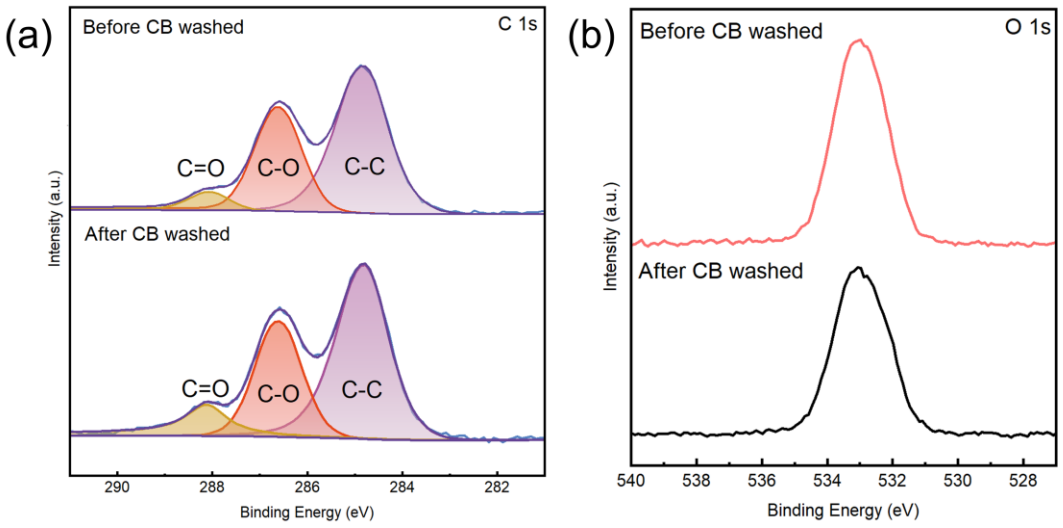

Fig. S6 XPS spectra of the (a) C 1s and (b) O 1s before and after CB washed.

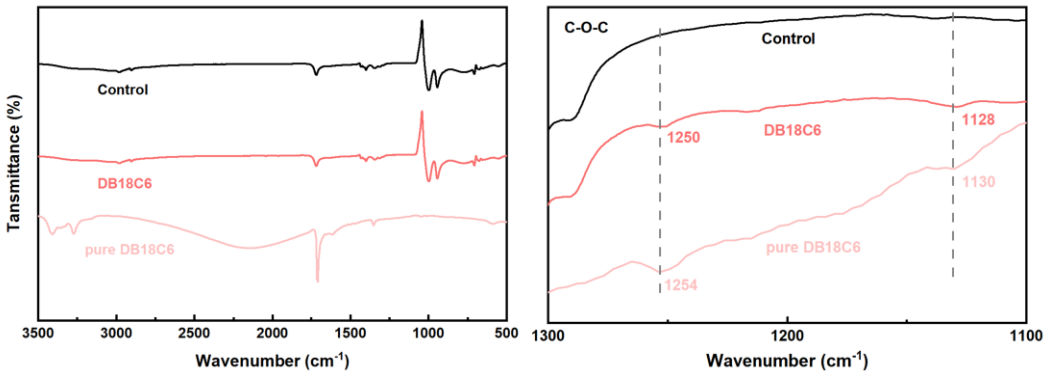

Fig. S7 FTIR spectra of control, DB18C6-modified and pure DB18C6 samples.

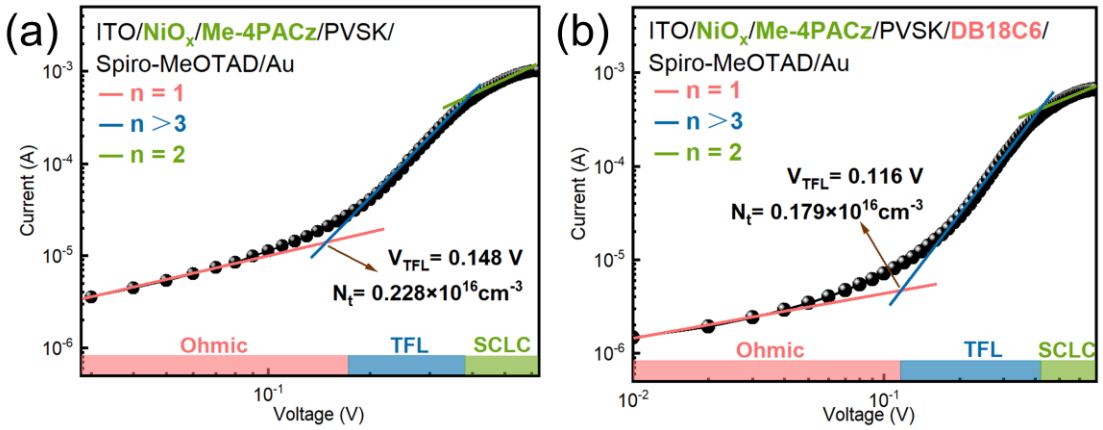

Fig. S8 The *I-V* curves of pure hole transport layer structure devices of (a) control and (b) target.

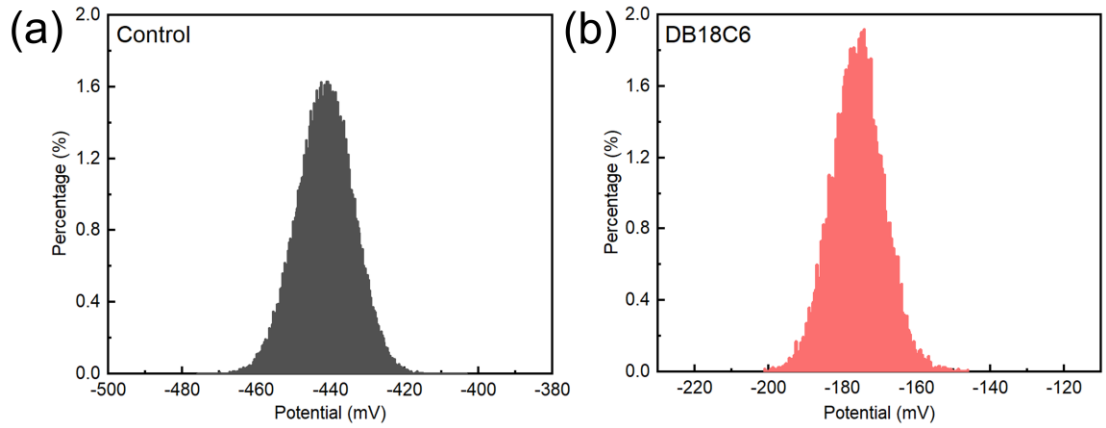

Fig. S9 The CPD distribution statistics extracted from KPFM of (a) control and (b) target films.

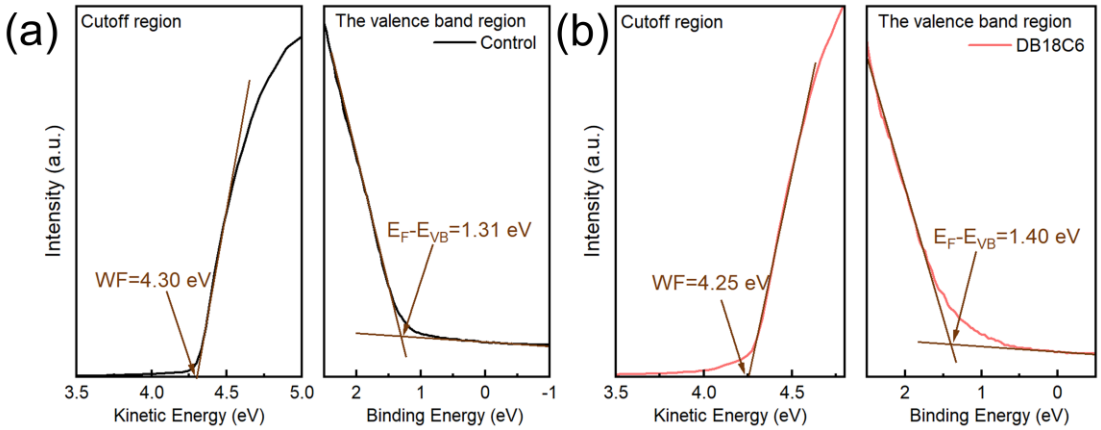

Fig. S10 UPS of (a) control and (b) target films.

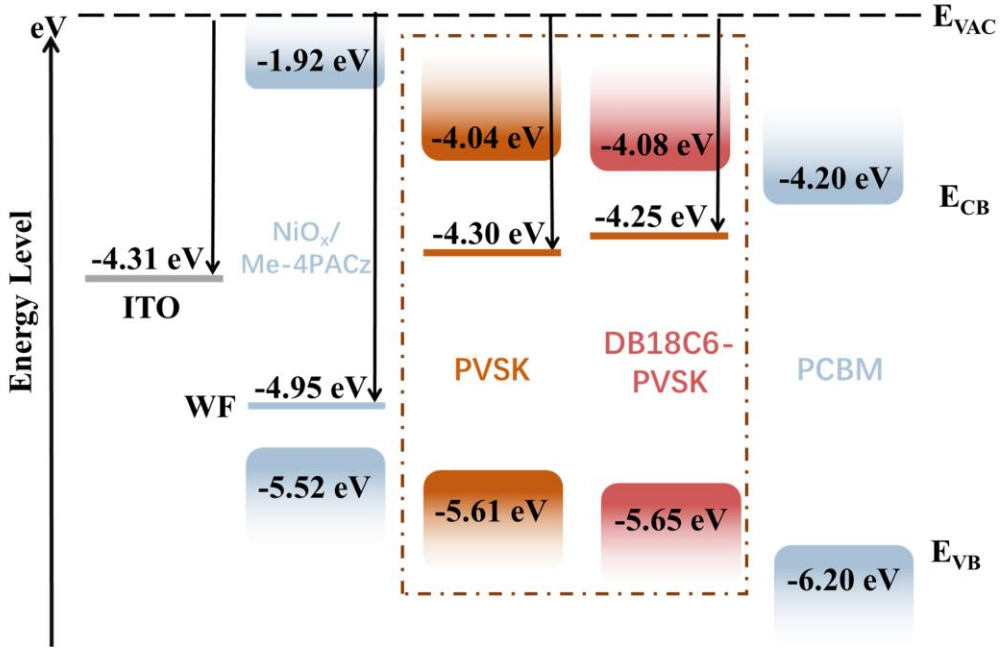

Fig. S11 The energy level alignment of each layer in inverted PSCs with control and target perovskite absorber.

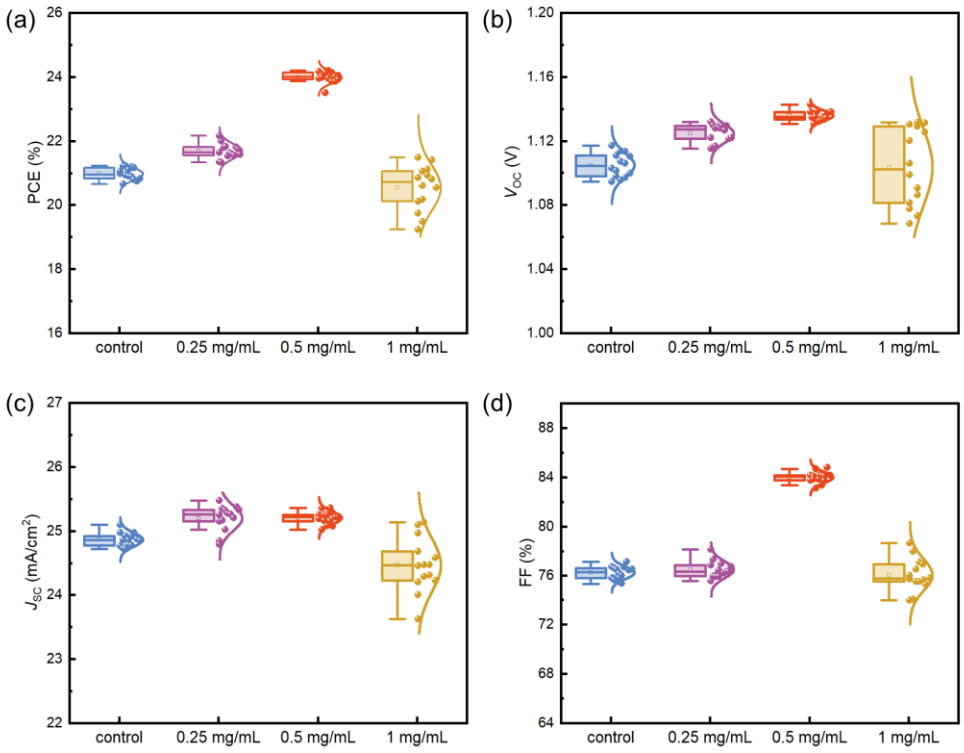

Fig. S12 Statistical box chart of (a) PCE, (b) V_{OC}, (c) J_{SC}, and (d) FF based on DB18C6 modified devices with different concentrations.

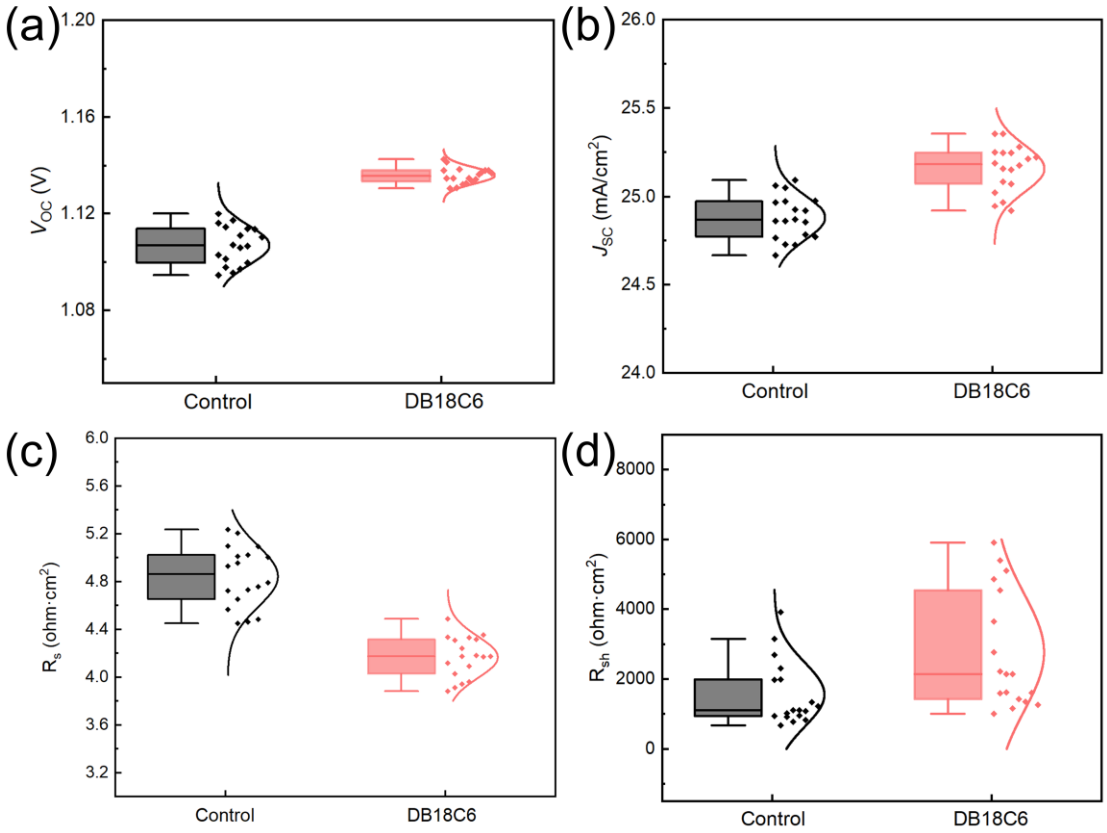

Fig. S13 Statistical box chart of (a) V_{OC}, (b) J_{SC} (c) series resistance (R_s) and (d) shunt resistance (R_{sh}) of control and target devices.

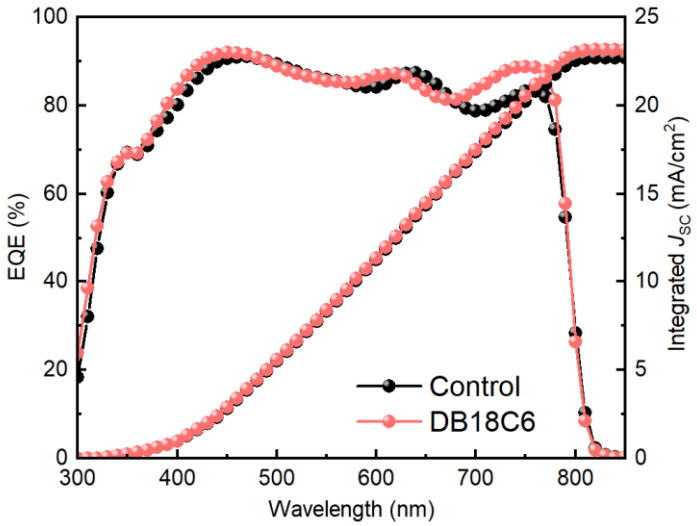

Fig. S14 EQE spectra of control and target devices.

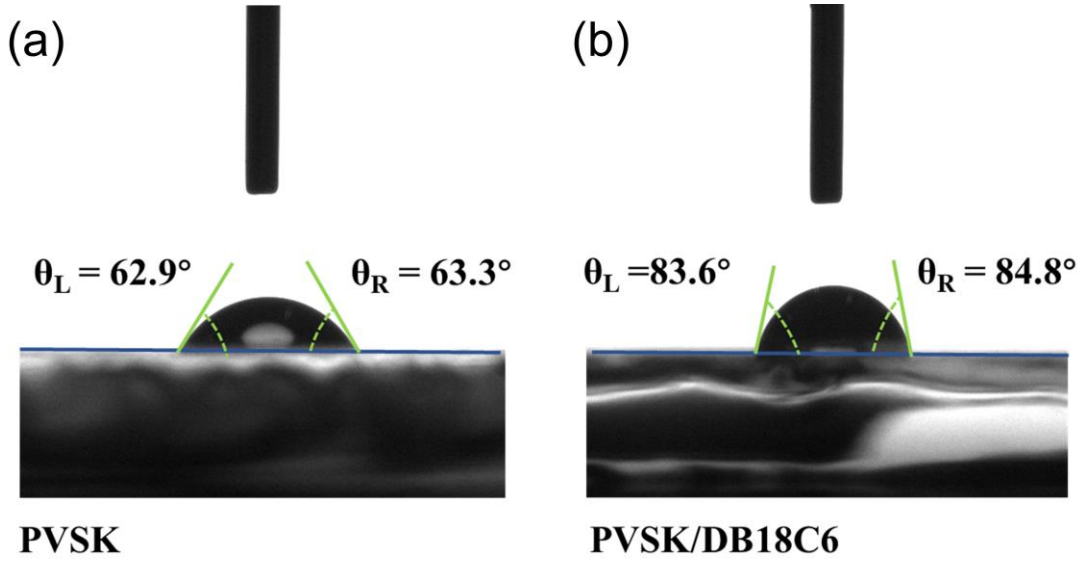

Fig. S15 Water contact angle of perovskite films: (a) control and (b) target.

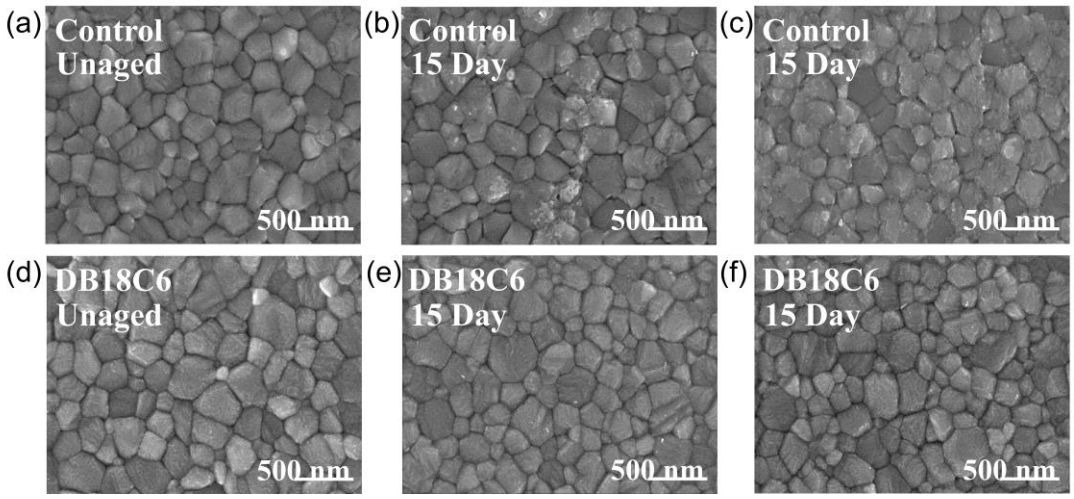

Fig. S16 Top-view SEM images of perovskite films: (a) unaged control, (b) and (c) aged for 15 days control, (d) unaged target, (d) and (e) aged for 15 days target.

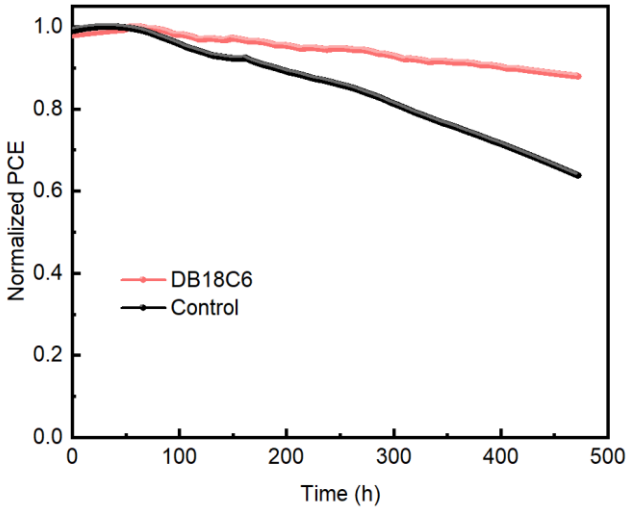

Fig. S17 The long-term operational stability of control and target devices.

Table S1 The FWHM of the main diffraction peaks in the XRD pattern of control and target films.

FWHM (°)	(001)	(011)	(002)	(012)	(022)
Control	0.15	0.18	0.18	0.21	0.19
Target	0.14	0.18	0.16	0.18	0.20

Table S2 TRPL fitting parameters of control and target films

	τ_1 (ns)	A_1 (%)	τ_2 (ns)	A_2	τ_{ave} (ns)
Control	47.39	0.65	1225.64	99.35	1225.14
Target	25.87	0.09	1753.72	99.91	1753.54

Table S3 Photovoltaic parameters of control and target PSCs.

Device		V_{OC} (V)	J_{SC} (mA/cm^2)	FF (%)	PCE (%)	HI
Control	Reverse scan	1.12	25.05	77.55	21.71	5.99
	Forward scan	1.11	24.98	73.60	20.41	
Target	Reverse scan	1.14	25.25	84.15	24.19	2.32
	Forward scan	1.14	25.21	81.90	23.63	